SUPPLEMENTAL METHODS

Flow Cytometry

Murine spleens were dissociated into single-cell suspensions using 70 μm nylon mesh strainers. RBCs were lysed using the ACK lysis buffer (ThermoFisher, #A1049201) for 3:30 minutes at room temperature followed by quenching with FACS buffer (PBS without Ca^{++}/Mg^{++}, 5% FBS, 2mM EDTA). Cells were then centrifuged (500 x g, 5 minutes, 4° C), resuspended, and re-filtered. Lymph nodes (inguinal and brachial) were dissociated into single-cell suspensions using microscope glass slides and filtered through 70 μm nylon mesh strainers. Cells were counted using the Beckman Coulter Vi-CELL XR 2.04. Cells were seeded in V-bottom 96-well plates on ice at a density of $2.5x10^5$ cells/well and first stained with a fixable viability dye (Zombie Violet Fixable Viability Kit, Biolegend, #423113, dilution 1:200). The following antibodies (all from Biolegend) were used: Brilliant Violet 605 anti-mouse CD274 (B7-H1, PD-L1) (#124321, clone 10F.9G2, dilution 1:200), FITC or APC anti-mouse CD19 (#152403 or #152409, clone 1D3/CD19, dilution 1:200), PerCP/Cyanine5.5 anti-mouse CD3 (#100218, clone 17A2, dilution 1:100), PE anti-mouse CD69 (#104507, clone H1.2F3, dilution 1:200), PE/Cyanine7 anti-mouse CD8α (#100722, clone 53-6.7, dilution 1:200), FITC anti-mouse CD45 (#103108, clone 30-F11, dilution 1:200), PE anti-mouse CD11b (#101207, clone M170, dilution 1:200), and APC/Cyanine7 anti-mouse CD4 (#100414, clone GK1.5, dilution 1:200). Fluorescence Minus One controls were generated for CD274 and CD69. Single stain controls were generated with UltraComp eBeads Compensation Beads (Invitrogen, #01222242). Flow cytometry data were acquired using the Thermo Fisher Attune NxT instrument at the Jonsson Comprehensive Cancer Center UCLA flow cytometry core and analyzed using the FlowJo software.

Single-cell RNA Sequencing Analysis

Freshly harvested splenocytes from three mice in each treatment group were pooled. Library preparation and sequencing were conducted at the UCLA Technology Center for Genomics and Bioinformatics (TCGB) core using the 10X Genomics 3' GEX kit (version 3). The control and diABZI-treated samples were sequenced using an Illumina sequencer and aligned to the mm10 mouse genome using CellRanger (version 4.0.0). The aligned datasets were processed with the Seurat (version 4.0.4) R package in R Studio (version 2021.09.1, R version 4.1.2) (*15*). For quality control, cells with greater than 20% mitochondrial gene expression and cells with a number of unique molecular identifiers (nUMI) lower than 200 were excluded. Features (genes) not supported by a minimum of 20 cells were excluded. The data from the control and treated samples were integrated using Seurat's IntegrateData function following their default processing pipeline. The integrated data were scaled;

any effects of the cell cycle on gene expression profiles were reduced by regressing out the CellCycle scores of each cell. We regressed the score differences between the S scores and G2M scores of each cell, which were computed using Seurat's CellCycleScoring function. Prior to the scoring, we converted Seurat's built-in human cell cycle genes to their murine counterpart using the biomaRt R package (*16*). We applied the principal component analysis (PCA) dimensionality reduction. Subsequently, based on the latter's top 30 principal components (PCs), we generated the Uniform Manifold Approximation and Projection (UMAP)-based visualization, nearest-neighbor computation, and cell clustering. Cluster-specific differentially expressed genes (DEGs), computed by Seurat's FindAllMarkers function, were used to identify the cell types of each cluster. Feature plots were generated using the FeaturePlot function (color contrast was increased by using the gene expression-specific color cutoffs for the 10th and 90th quantiles). To generate the overview of the relative breakdown of cluster composition in each condition, the dittoBarPlot function from the dittoSeq R package was used. We obtained treatment-specific DEGs by applying the FindMarkers function on the control and treated cell subsets of each cluster. DEGs specific to glycolysis were visualized by generating a heatmap of average log2 fold change values (from Seurat's FindMarkers function) in R. To generate a heatmap of ontological analysis, the built-in Seurat function for EnrichR (DEenrichRPlot) was used to analyze the top 100 DEGs against the MSigDB Hallmark 2020 gene sets. Single-cell RNA sequencing analysis was also performed using Elucidata's Polly software packages (www.elucidata.io, Elucidata, Cambridge, MA).

SUPPLEMENTAL FIGURE LEGENDS

SUPPLEMENTAL FIGURE 1. ScRNAseq annotation of cell clusters and expression of glycolytic genes across splenocytes from control and systemic STING agonist-treated mice. (**A**) UMAP projection of the expression profiles of the 11,082 splenocytes color-coded for the indicated cell type in both groups. (**B**) The proportions of cells in each cell cluster among all splenocytes identified. (**C**) Heatmap showing the expression of genes involved in glycolysis.

SUPPLEMENTAL FIGURE 2. Validating specific immune cell populations with induced ^{18}F-FDG uptake following systemic STING agonist treatment. (**A**) Experimental scheme. (**B–D**) *Ex vivo* quantification of ^{18}F-FDG uptake in intact spleens (**B**), splenocytes after single cell suspensions (**C**), and enriched T and B lymphocyte subsets (**D**) from STING agonist-treated mice after 24 hr. The mice were injected with 9.25 MBq ^{18}F-FDG and sacrificed 1 h later for indicated gamma counter analyses; n = 5 mice/group.

SUPPLEMENTAL FIGURE 3. Immune activation markers induced along with increase ^{18}F-FDG uptake following systemic STING activation. (**A**) Representative ^{18}F-FDG-PET scans of control and STING agonist-treated C57BL/6 mice with indicated doses of diABZI at 24 h. Mice were injected with 0.74 MBq ^{18}F-FDG followed by PET imaging 1 h later. (**B**) *Ex vivo* gamma counter measurements of ^{18}F-FDG accumulation in spleen and lymph nodes (combined inguinal and brachial) isolated from mice. Mice were injected with 9.25 MBq ^{18}F-FDG followed by gamma counter measurements; n = 3-4 mice/group. (**C**) *Ex vivo* gamma counter measurements of ^{18}F-FDG accumulation in splenocytes. (**D**) Representative flow histograms of CD69 and PD-L1 expression pre-gated for CD4$^+$, CD8$^+$, or the B cell lineage marker CD19 (top panels) and summarized in bar plots (bottom panels); n = 3-4 mice/group.

SUPPLEMENTAL FIGURE 4. Changes in ^{18}F-FDG uptake in lymph nodes following systemic STING activation correlate with the upregulation of immune activation and inhibitory markers by T and B lymphocytes. (**A**) Percent CD69 and PD-L1 levels in each immune cell subset pre-gated for CD4$^+$, CD8$^+$, or the B cell lineage marker CD19 from isolated lymph nodes. (**B**) Scatterplots showing the correlation of log-transformed *ex vivo* ^{18}F-FDG uptake (x-axis) and CD69 and PD-L1 expression on CD8$^+$ T cells (y-axis) isolated from lymph nodes. Spearman correlation is indicated for CD8$^+$ T cells in the graph while CD4$^+$ T cells and B cells are in the table.

SUPPLEMENTAL FIGURE 5. Increased splenic ^{18}F-FDG uptake in systemic STING agonist-treated mice does not require interferon signaling. (**A–B**) *Ex vivo* gamma counter measurements of ^{18}F-FDG accumulation in splenocytes (**A**) and enriched splenic immune cells (**B**) of control and STING agonist-treated

Ifnar KO mice; n = 4–5 mice/group. (**C**) Percent CD69 and PD-L1 levels in each immune cell subset pre-gated for $CD4^+$, $CD8^+$, or the B cell lineage marker CD19 from isolated spleen; n = 5–6mice/group.

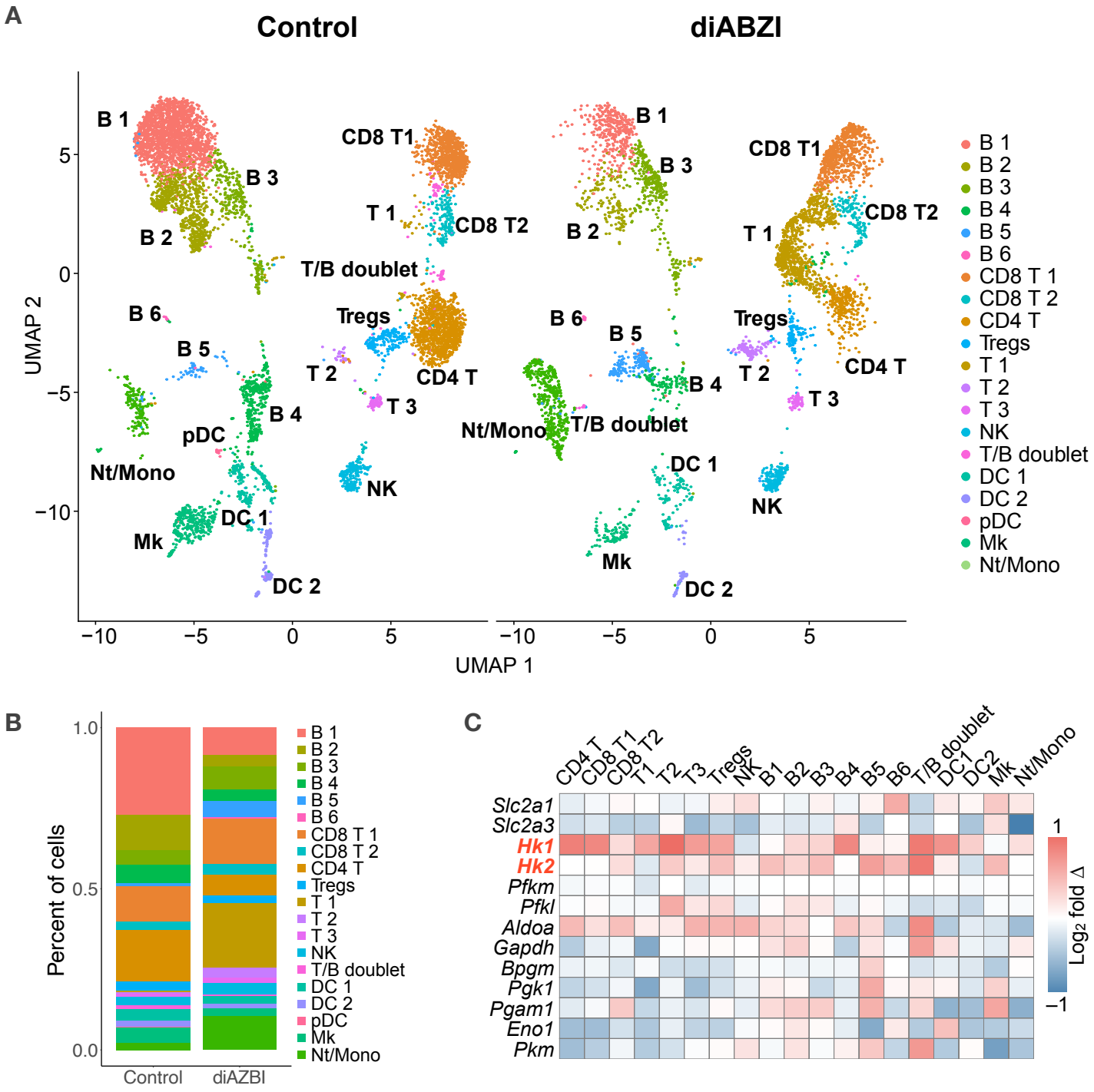

SUPPLEMENTAL FIGURE 1. ScRNAseq annotation of cell clusters and expression of glycolytic genes across splenocytes from control and systemic STING agonist-treated mice. (**A**) UMAP projection of the expression profiles of the 11,082 splenocytes color-coded for the indicated cell type in both groups. (**B**) The cell cluster proportions among all splenocytes identified. (**C**) Heatmap showing the expression of genes involved in glycolysis.

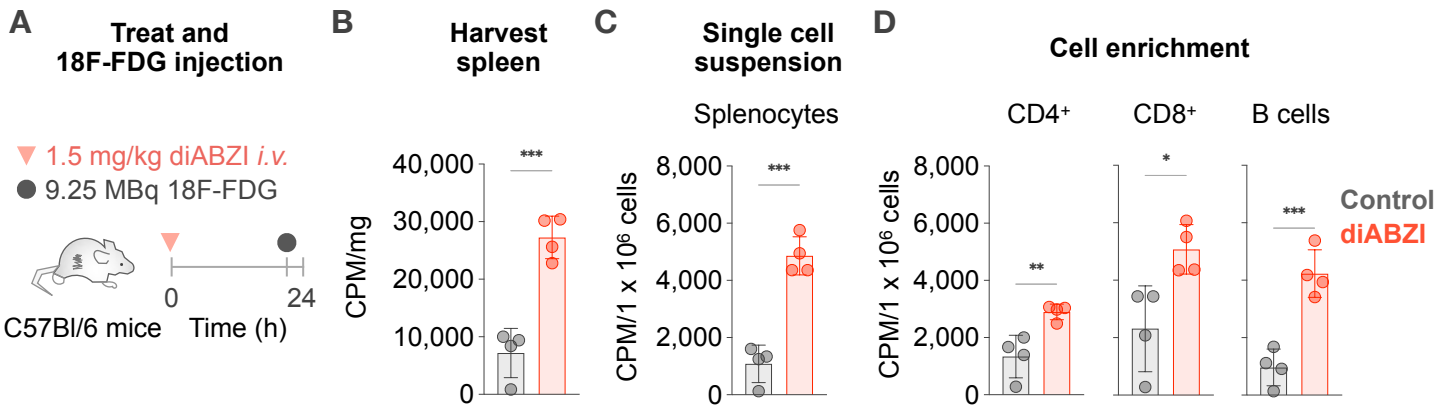

SUPPLEMENTAL FIGURE 2. Validating specific immune cell populations with induced ^{18}F-FDG uptake following systemic STING agonist treatment. (**A**) Experimental scheme. (**B–D**) *Ex vivo* quantification of ^{18}F-FDG uptake in intact spleens (**B**), splenocytes after single cell suspensions (**C**), and enriched T and B lymphocyte subsets (**D**) from STING agonist-treated mice after 24 hr. The mice were injected with 9.25 MBq ^{18}F-FDG and sacrificed 1 h later for indicated gamma counter analyses; n = 5 mice/group.

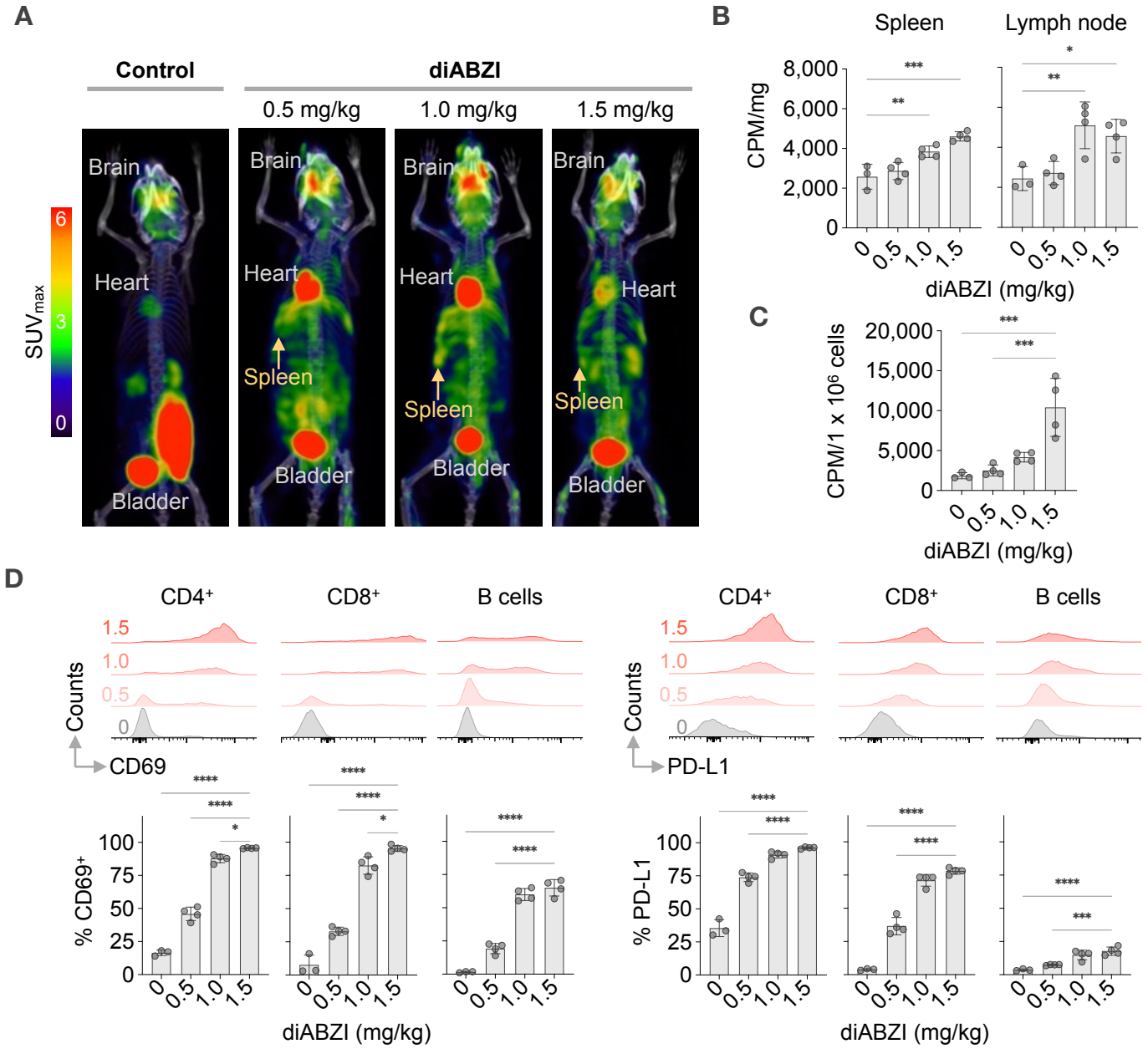

SUPPLEMENTAL FIGURE 3. Immune activation markers induced along with increase ^{18}F-FDG uptake following systemic STING activation. (**A**) Representative ^{18}F-FDG-PET scans of control and STING agonist-treated C57BL/6 mice with indicated doses of diABZI at 24 h. Mice were injected with 0.74 MBq ^{18}F-FDG followed by PET imaging 1 h later. (**B**) *Ex vivo* gamma counter measurements of ^{18}F-FDG accumulation in spleen and lymph nodes (combined inguinal and brachial) isolated from mice. Mice were injected with 9.25 MBq ^{18}F-FDG followed by gamma counter measurements; n = 3-4 mice/group. (**C**) *Ex vivo* gamma counter measurements of ^{18}F-FDG accumulation in splenocytes. (**D**) Representative flow histograms of CD69 and PD-L1 expression pre-gated for CD4$^+$, CD8$^+$, or the B cell lineage marker CD19 (top panels) and summarized in bar plots (bottom panels); n = 3-4 mice/group.

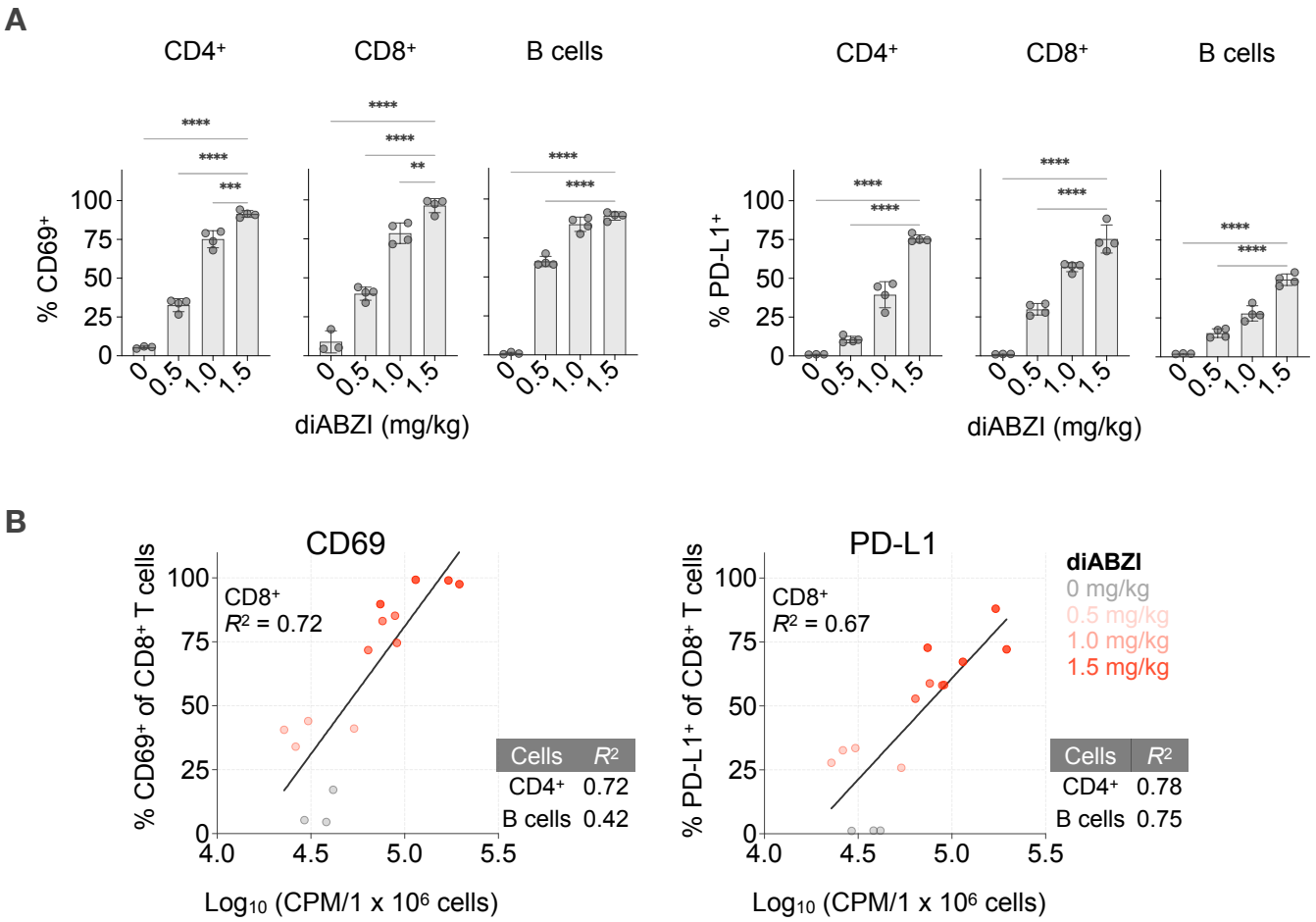

SUPPLEMENTAL FIGURE 4. Changes in ^{18}F-FDG uptake in lymph nodes following systemic STING activation correlate with the upregulation of immune activation and inhibitory markers by T and B lymphocytes. (**A**) Percent CD69 and PD-L1 levels in each immune cell subset pre-gated for CD4$^+$, CD8$^+$, or the B cell lineage marker CD19 from isolated lymph nodes. (**B**) Scatterplots showing the correlation of log-transformed *ex vivo* ^{18}F-FDG uptake (x-axis) and CD69 and PD-L1 expression on CD8$^+$ T cells (y-axis) isolated from lymph nodes. Spearman correlation is indicated for CD8$^+$ T cells in the graph while CD4$^+$ T cells and B cells are in the table.

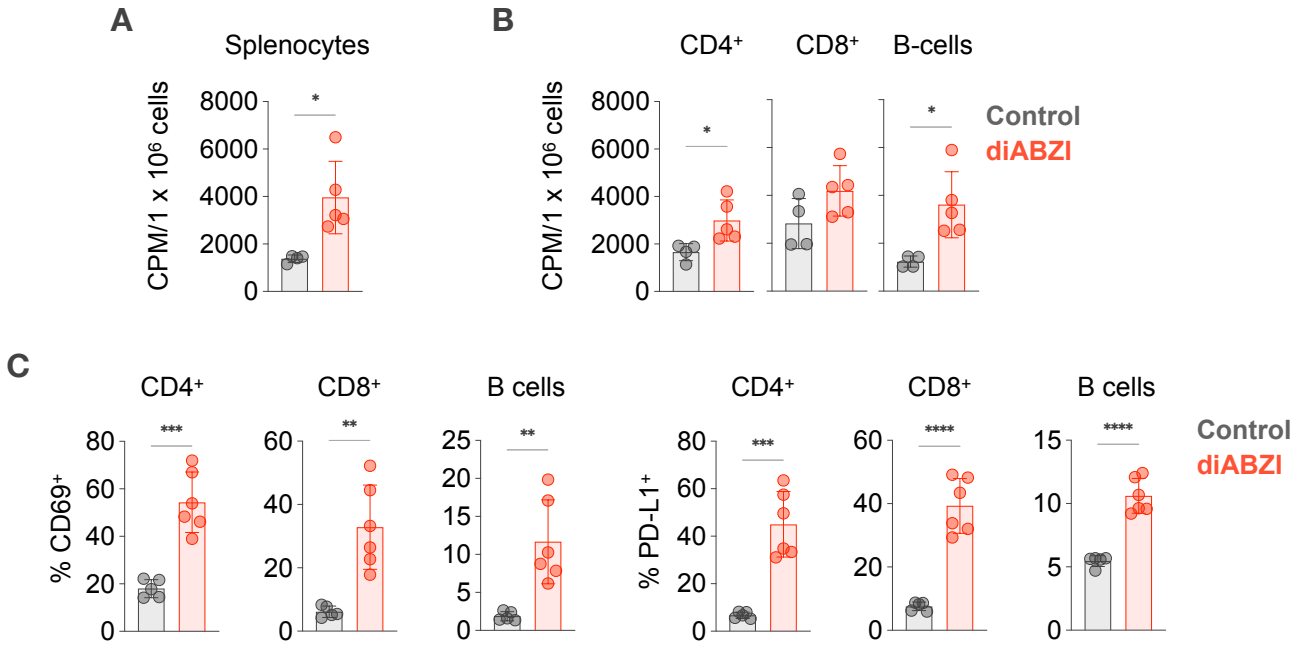

SUPPLEMENTAL FIGURE 5. Increased splenic ^{18}F-FDG uptake in systemic STING agonist-treated mice does not require interferon signaling. (**A–B**) *Ex vivo* gamma counter measurements of ^{18}F-FDG accumulation in splenocytes (**A**) and enriched splenic immune cells (**B**) of control and STING agonist-treated *Ifnar* KO mice; n = 4–5 mice/group. (**C**) Percent CD69 and PD-L1 levels in each immune cell subset pre-gated for CD4$^+$, CD8$^+$, or the B cell lineage marker CD19 from isolated spleen; n = 5–6mice/group.